The photophysics of naphthalene dimers controlled by sulfur bridge oxidation

Clàudia Climent, Mario Barbatti, Michael O Wolf, Christopher J Bardeen, David Casanova

▶ **To cite this version:**

Clàudia Climent, Mario Barbatti, Michael O Wolf, Christopher J Bardeen, David Casanova. The photophysics of naphthalene dimers controlled by sulfur bridge oxidation. Chemical Science, 2017, 8 (7), pp.4941-4950. 10.1039/C7SC01285C . hal-02288763

HAL Id: hal-02288763

https://amu.hal.science/hal-02288763

Submitted on 16 Sep 2019

HAL is a multi-disciplinary open access archive for the deposit and dissemination of scientific research documents, whether they are published or not. The documents may come from teaching and research institutions in France or abroad, or from public or private research centers.

L'archive ouverte pluridisciplinaire **HAL**, est destinée au dépôt et à la diffusion de documents scientifiques de niveau recherche, publiés ou non, émanant des établissements d'enseignement et de recherche français ou étrangers, des laboratoires publics ou privés.

Photophysics of Naphthalene Dimers Controlled by the Sulfur Bridge Oxidation

Clàudia Climent[a], Mario Barbatti[b], Michael O. Wolf[c], Christopher J. Bardeen[d], David Casanova[e,f,*]

[a]Departament de Ciència de Materials i Química Física and Institut de Química Teòrica i Computacional (IQTCUB), Universitat de Barcelona, Martí i Franquès 1-11, Barcelona 08028, Spain.
[b]Aix Marseille Univ, CNRS, ICR, Marseille, France.
[c]Department of Chemistry, University of British Columbia, 2036 Main Mall, Vancouver, BC, V6T 1Z1, Canada.
[d]Department of Chemistry, University of California Riverside, 501 Big Springs Road, Riverside, California 92521, United States.
[e]Kimika Facultatea, Euskal Herriko Unibertsitatea (UPV/EHU), Donostia International Physics Center, Paseo Manuel de Lardizabal, 4, Donostia 20018, Spain.
[f]IKERBASQUE, Basque Foundation for Science, Bilbao 48013, Spain.

Abstract

In this study we investigate in detail the photophysics of naphthalene dimers covalently linked by a sulfur atom. We explore and rationalize how the oxidation state of the sulfur-bridging atom directly influences the photoluminescence of the dimer by enhancing or depriving radiative and non-radiative relaxation pathways. In particular, we discuss how oxidation controls the amount of electronic transfer between naphthalene moieties and the participation of the SO_n bridge in the low-lying electronic transitions. We identify the sulfur electron lone-pairs as crucial actors in the non-radiative decay of the excited sulfide and sulfoxide dimers, which are predicted to go via a conical intersection (CI). Concretely, two types of CI have been identified for these dimers, which we associate with photo-induced pyramidal inversion and reverse fragmentation mechanisms in aryl sulfoxide dimers.

The obtained results and conclusion are general enough to be extrapolated to other sulfur-bridged conjugated dimers, therefore proportionating novel strategies in the design of strong photoluminescence organic molecules with controlled charge transfer.

1. Introduction

Organic photovoltaics (OPVs) represent a very promising alternative in the conversion of solar energy to electricity. Although OPVs have the potential to provide electricity at a lower cost than solar technologies of the first and second generation, current record efficiencies (~13%)[1] are still far too low to compete with the performance of silicon panels[2] and other non-fossil energy sources. Organic solar cells present many advantages, i.e. abundance of materials, well-developed organic chemistry for their synthesis, available chemical strategies to tune their properties and can be produced as thin, flexible and light modules that can be easily manufactured at room temperature. But, in order for OPV technology to compete with other energy sources some fundamental obstacles need to be overcome. In particular, OPV technologies exhibit short device lifetimes and low dielectric constants, resulting in low energy conversion efficiencies. One of the fundamental issues at the microscopic level is the generation of separated charges from the optical exciton. High exciton binding energies result in energy losses at the cell heterojunction that induce rather low open-circuit voltages (V_{OC}). A promising and elegant strategy to increase V_{OC} in OPVs is the use of symmetric molecular electron acceptors, such as covalent dimers of organic chromophores (bichromophores), able to undergo symmetry-breaking charge transfer (SBCT).[3-5] In SBCT, the initial excitation generated by photo-absorption relaxes to an intramolecular charge transfer state that breaks the molecular symmetry. Then, electron CT at the donor/acceptor interface generates an oxidized donor and reduced acceptor separated by a neutral chromophore, preventing fast charge recombination. Organic bichromophores have also been proposed as highly emissive molecules to use in organic light emitting devices (OLEDs)[6,7] as an alternative to large aromatic molecules. In addition to strong photoluminescence (PL), optimal molecular systems to be used in OLEDs must allow intermolecular CT.[8]

The range of applicability of bichromophores is expected to be related to the nature of the bridged monomers and how they interact. The electronic coupling between the conjugated moieties depends on the geometry and electronic structure of the covalent linker, and understanding the parameters that ultimately control and determine such interactions becomes critical to design molecular systems with the desired characteristics. Recently, it was shown that the covalent linkage between conjugated chromophores by a sulfur bridge has a large impact on the fluorescence efficiencies of the parent chromophores, with a large increase of PL yield with oxidation of the bridging sulfur atom, indicating a clear strategy in the search of strong molecular emitters.[9] This trend was later scrutinized for the case of terthiophene dimers.[10] That study concluded that rapid intersystem crossing (ISC) to the triplet state

manifold is the main deactivation process limiting the fluorescence quantum yield, as observed in pristine terthiophene.[11,12] The ISC efficiency is reduced in the presence of intramolecular charge transfer (CT), which can be tuned by the oxidation state of the bridging sulfur group. Electron lone-pairs on the sulfur atom screen the electronic interaction between the two chromophores, decreasing CT and allowing efficient ISC for the sulfide and sulfoxide dimers, and resulting in larger PL efficiency for the sulfone bridge with no electron lone-pairs on S.

Despite the much less efficient ISC expected for naphthalene due to molecular planarity and the lack of sulfur atoms, PL in SO_n bridged naphthalene dimers exhibit the same trend as in the terthiophene analogues. Hence, in order to understand the origin of such behavior and to further explore the validity of the lone-pair screening concept, the present study features the photophysical properties of naphthalene covalent dimers linked through the SO_n bridge with n = 0, 1 and 2. Throughout this paper we label these three molecules as **D0** (sulfide), **D1** (sulfoxide) and **D2** (sulfone).

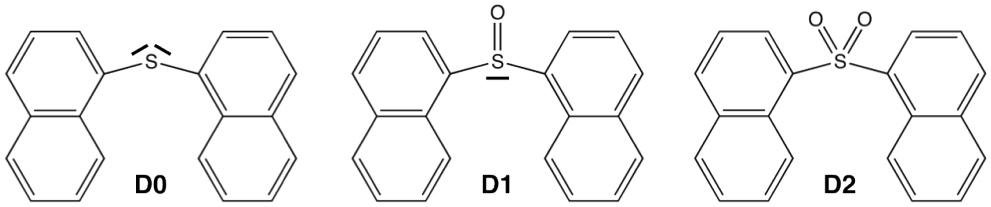

Scheme 1. Molecular representation of **Dn** dimers. Sulfur electron lone pairs are explicitly indicated.

The work is organized as follows. First we discuss the relative stability of structural conformers of **Dn** dimers and potential interconversion paths. Then we explore the nature of the low-lying singlet states for the most stable conformers and the structural and electronic properties of local minima on the excited state energy surface. Finally, we discuss the availability of non-radiative decay pathways from the lowest excited singlet to the ground state.

2. Computational details

Electronic structure calculations for ground and excited states were performed within the framework of density functional theory (DFT)[13,14] and its time-dependent version (TDDFT),[15,16] respectively. To take into account weak interactions and important electronic redistribution between the naphthalene moieties and the SO_n bridge upon photoexcitation the ωB97X-D functional[17] was used together with the 6-31+G(d) basis set.[18-20] Investigations on the dependence of the energy functional and basis set can be found as Supporting Information (Tables S1 and S2). Dichloromethane (DCM) solvent effects were taken into account with the

polarizable continuum model using the integral equation formalism variant (IEFPCM).[21,22] Critical points on the ground state potential energy surface (PES) were optimized with no restrictions and characterized within the harmonic approximation. The simulated emission spectra were calculated by convolution of Gaussian functions (half-bandwidth of 2500 cm^{-1}) centered at the computed vertical emission energies of all excited state minimum and were averaged according to ground or excited state Boltzmann populations (based on relative electronic energies). Computation of diabatic states was obtained by means of the Edmiston-Ruedenberg localization scheme.[23] Energy crossing points and derivative couplings between S_0/S_1 were computed at the spin-flip DFT (SF-DFT) approximation[24] with the BHHLYP functional.[25,26]

All calculations were performed with the Gaussian09 package, revisions B01 and D01,[27] and the Q-Chem program.[28]

3. Results and discussion

3.1. Thermal conformers

The rotation around the S-naphthalene bonds of **Dn** dimers results in different structural conformers, which are local minima on the ground state PES (Figures 1 and S1).

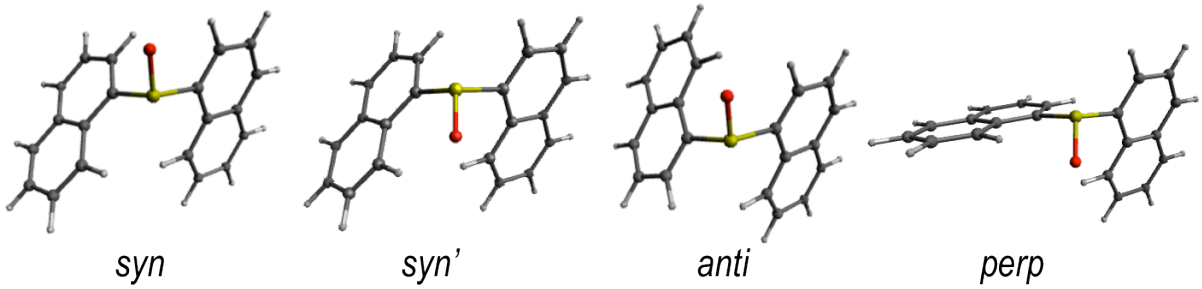

Figure 1. Lowest energy conformers for the ground state of **D1** dimer in DCM solution. Low energy conformers of **D0** and **D2** are shown in Figure S1.

The energetically lowest forms of **D0** and **D1** in solution correspond to *syn* and *anti* arrangements of the naphthalene units with *syn* being slightly lower in energy (Table 1). As a result, it is reasonable to expect both conformers to be present in solution as computed by their Boltzmann fractions. On the other hand, **D2** shows a clear preference for the *anti* conformer, which is expected to largely be the main form in DCM solution.

It is worth noting that while **D0** only shows some sizeable net charge in any of its parts, i.e. the two naphthalene and sulfur bridge in its *anti* conformer, the polarity of the S-O bond in the sulfoxide and sulfone bridges induces an electronic distribution towards the more electronegative O atoms (Table 1). Charge polarization in **D1** basically affects the SO linker, with S and O atoms carrying positive and negative charges, respectively. The presence of two

O atoms in **D2** is able to pull considerable electron density from the two naphthalene units in the *syn* and *anti* conformers, resulting in a positive net charge on each chromophore. The different behavior of the *perp* form is related to the orthogonal orientation between naphthalene units, which results in asymmetrically charged chromophores.

Table 1. Relative energies ΔE (in kcal/mol), relative Boltzmann population at T = 298K (Pop. in %) and Mulliken charges (q) on the S and O atoms, and on the naphthalene moieties for the ground state optimized structures of the lowest energy conformers (*conf.*) of **D0**, **D1** and **D2** dimers in DCM.

dimer	*conf.*	ΔE	Pop.	q(S)	q(O_n)	q($Napth_2$)
D0	*syn*	0.0	74	0.00	-	0.00
	anti	0.7	23	0.20	-	-0.20
	anti'	1.8	3	-0.04	-	0.04
D1	*syn*	0.0	69	0.68	-0.69	0.01
	syn'	3.5	<1	0.48	-0.69	0.21
	anti	0.5	30	0.68	-0.71	0.03
	perp	2.8	<1	0.54	-0.69	0.14
D2	*syn*	2.5	1	0.18	-0.97	0.79
	anti	0.0	94	0.27	-0.95	0.68
	perp	1.8	5	0.92	-0.99	0.08

In addition to identifying and characterizing the most stable conformations of the naphthalene dimers, it is also important to quantify the barriers for their interconversion. The structural transformation between the low energy conformers of each dimer can be achieved by the torsion of one naphthalene moiety with respect to the other one. The ground state energy profiles of such mechanisms are shown in Figures S2-S4. The computed barriers for the molecular torsion between the low-lying conformers are in the 2-6 kcal/mol range, indicating slow thermal conversion at room temperature.

In addition to the torsion mechanism, the conversion between conformers of **D1** can be achieved by pyramidal inversion of the S atom (Figure 2). The transition states for the inversion of the *syn* and *anti* conformers exhibit a planar geometry around the sulfur atom with a naph-S-naph angle close to 120°, i.e. corresponding to a trigonal planar geometry, and much larger than the ground state angle (close to the tetrahedral angle). The computed inversion barriers for the *syn*→*syn'* and *anti*→*anti* conformational pathways are 38.4 and 38.6 kcal/mol, respectively, in quantitative agreement with computational estimations of the pyramidalization barrier computed for H_2SO, DMSO[29] and related sulfoxide heterodimers.[30] Hence, thermal pyramidal inversion of the sulfoxide dimer is expected to be very slow, as it has been previously observed for the racemization of aryl sulfoxides.[31,32] Analogously to the pyramidal inversion in **D1**, the *syn* and *anti* conformers of the **D2** dimer might convert to

themselves by a tetrahedral inversion through the planarization of the sulfone center with a square planar transition state. Our calculations indicate that such geometry lies very high in energy (97 kcal/mol with respect to the ground state *anti* conformer) and hence thermal interconversion of sulfone-bridged naphthalene dimer via planarization can be completely disregarded. In spite of the lack of oxygen atoms in the **D0** bridge, it can also experience a similar inversion of the molecular structure by increasing the naph-S-naph bent angle at the bridge from the tetrahedral-like value (105°) in the *syn* and *anti* ground state minima to the linear C-S-C disposition. Again, the computational estimation of the energy barrier for the structural inversion of **D0** is too high (70 kcal/mol) to be thermally available, in very good agreement to the linearization energy estimated for H_2S.[33]

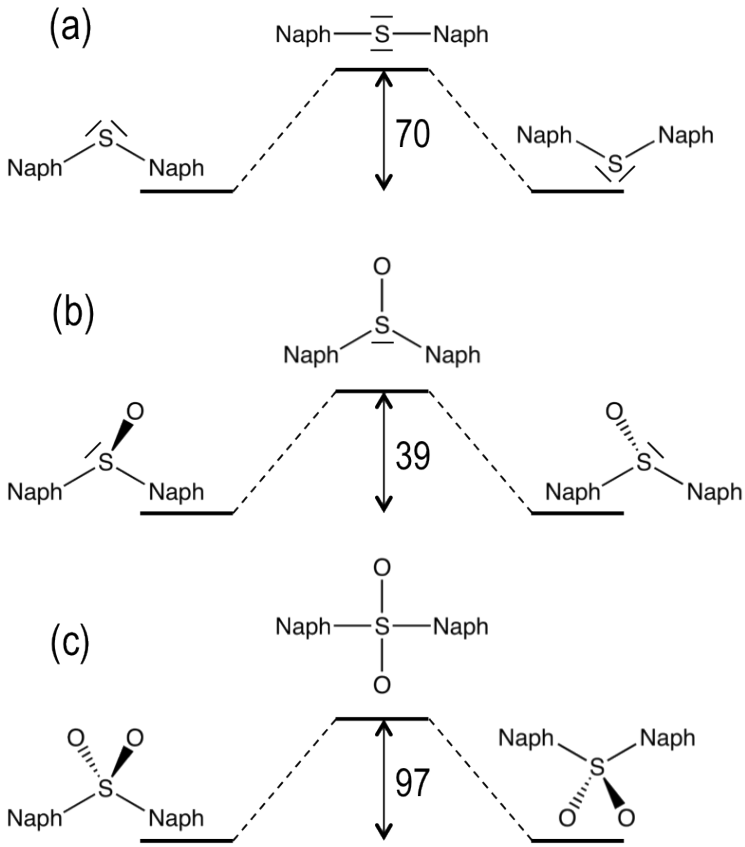

Figure 2. Ground state transition energy barriers (in kcal/mol) for the structural inversion of **D0** (a), **D1** (b) and **D2** (c) dimers. Molecular representations are only meant to indicate the main differences between S_0 and TS geometries. The nature of the S-O bond (single or double bond) has been omitted for the sake of clarity.

3.2. Photoabsorption

Computed vertical excitation energies from the ground state to the lowest excited singlet state of the **Dn** dimers are rather close to each other regardless of the oxidation state of the sulfur bridge and lie within the 4.2-4.4 eV range, in fairly good agreement with

experimental absorption maxima measured in DCM solution (Table 2). Moreover, transition energies and oscillator strengths show small variations between different conformers.

Table 2. Vertical transition energies ΔE (in eV), oscillator strength (*f*), electronic character (in %) LE (on naphthalene fragments), CT (between naphthalene moieties) and CT_B (from the SO_n bridge to the naphthalenes) and electronic couplings between the lowest LE, CT and CT_B diabatic states (in meV) for the lowest excited singlet of the most stable conformers of **D0**, **D1** and **D2** dimers computed at the ωB97X-D/6-31+G(d) level.

dimer	*conf.*	ΔE[a]	*f*	LE	CT	CT_B	LE/CT	LE/CT_B
D0	*syn*	4.24	0.335	37	14	49	102	509
	anti	4.31	0.326	59	5	36	65	244
D1	*syn*	4.41	0.301	84	1	15	129	200
	anti	4.43	0.312	91	1	8	126	195
D2	*anti*	4.42	0.272	96	4	0	162	N/A

[a]Experimental absorption maxima: 4.11 eV (**D0**), 4.19 eV (**D1**) and 4.16 eV (**D2**).[9]

The main contribution to the lowest electronic transition from the most stable conformations (*syn* and *anti*) of naphthalene dimers corresponds to the single electron promotion from the two highest occupied molecular orbitals (HOMO and HOMO-1) to the two lowest unoccupied molecular orbitals (LUMO and LUMO+1). The frontier orbitals are mostly delocalized over the two naphthalene moieties with some contribution of the SO_n bridge, mainly for the HOMOs of **D0** and **D1** molecules (Figure 3).

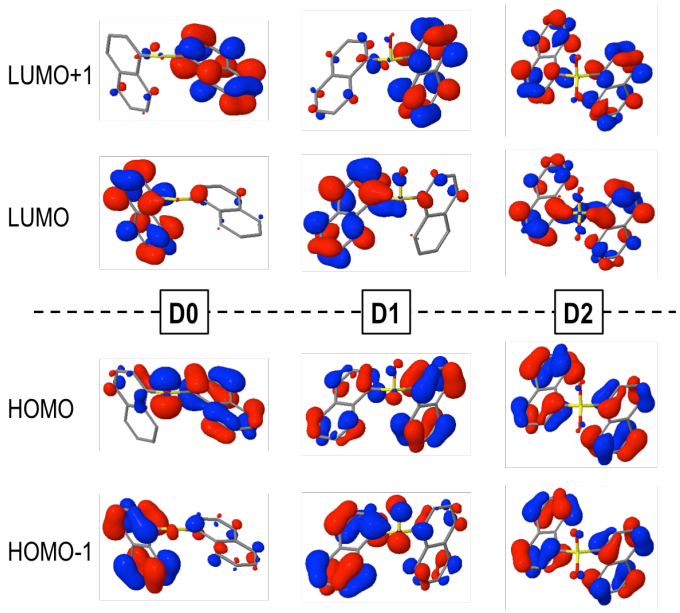

Figure 3. HOMOs (bottom) and LUMOs (top) of *syn*-**D0** (left), *syn*-**D1** (middle) and *anti*-**D2** (right) dimers computed in DCM solution.

Despite the similarities between excitation energies and oscillation strengths of the $S_0 \rightarrow S_1$ transition in **D0**, **D1** and **D2** dimers, detailed electronic structure analysis brings to

light significant differences in the nature of the transition upon oxidation of the bridge (Table 2). Decomposition of the electronic transition in terms of diabatic states corresponding to local excitations (LE) on the naphthalene moieties, charge transfer excitations between the aryl fragments (CT) and electronic transition from the bridge to the naphthalene chromophores (CT_B) highlights important differences in the nature of the vertical excitation upon oxidation of the sulfur atom linker (Table 2). In general, the main contribution corresponds to $\pi \rightarrow \pi^*$ excitations on both naphthalene moieties, especially for the sulfone case. This contribution accounts for ~90% of the transition in **D1** and has proportionally a much lower role in the excitation of the **D0** conformers. This decrease of naphthalene-centered excitations is related to the larger involvement of the SO_n orbitals in the transition, corresponding to the electron lone pairs on the sulfur (**D0** and **D1**) and on oxygen (**D1**) atoms, i.e. *n*(S) and *n*(SO) respectively. The presence of electron lone-pairs in the sulfide and sulfoxide linkers allows for sizeable CT_B contributions, related to the different electron density distributions found in the HOMOs (Figure 3). CT_B contributions are already rather important in **D1** (15% in the lowest *syn* conformer) and become the main contribution in *syn*-**D0** (49%). On the other hand, the lack of available lone-pairs forbids the bridge-to-naphthalene electronic transitions in the S_1 state of **D2**. For most of the cases, charge transfer between the two naphthalene fragments (CT) plays a minor role in the lowest excitation of **Dn** dimers. It is worth noticing that the LE/CT electronic coupling increases with the number of oxygen atoms in the bridge. This trend can be attributed to the electronic screening by the sulfur electron lone-pairs, that limits the interaction between the two sets of π-electrons, as recently discussed in sulfur-bridged terthiophene dimers.[10] On the other hand LE/CT_B couplings are much larger in the sulfide than in the sulfoxide bridge in accordance with the amount of CT_B in the excitation, which can be rationalized as a result of the presence of one additional electron lone-pair in the former.

3.3. Fluorescent emission

Thorough computational searches of local minima on the lowest excited state PES of naphthalene dimers identifies a variety of states susceptible to decay back to the ground state via fluorescence emission (Table 3). The **Dn** dimers exhibit different structurally relaxed states corresponding to the stabilization of $\pi \rightarrow \pi^*$ excitations either localized on one naphthalene unit (L) or delocalized over both conjugated chromophores (D), or to the optimization of CT excitations from the SO_n bridge (for n = 0 and 1) to the π^* naphthalene empty orbitals (CT_B). The lack of sulfur lone-pairs prohibits the stabilization of CT_B states on

the S_1 PES of **D2**, in line with the decomposition of the lowest excitation at the Franck-Condon (FC) geometry (Table 2).

The *syn*-**Dn** dimers hold excited state minima with excimeric nature and molecular geometries with the two naphthalene units close to the coplanar eclipsed relative orientation (Figure S5). These states present the largest Stokes shift for each dimer and are built as naphthalene $\pi\rightarrow\pi^*$ excitations delocalized over the two chromophores without any involvement of the sulfur bridge. In addition, the large weights of CT excitations (50% of the transition) for these states unequivocally identify them as naphthalene excimers (Figure S6). It is worth noting that while in **D0** the excimer is the energetically highest optimized excited state conformer, it is the most stable state in **D1** and **D2**, with larger interstate gaps in the latter. Moreover, the adiabatic energy gap with respect to the ground state *syn* conformer decreases as **D0** > **D1** > **D2**, indicating stronger excimer stabilization for higher oxidation states of the bridge. The LE/CT couplings for the three *syn* excimers are computed at 626 (**D0**), 643 (**D1**) and 707 (**D2**) meV, considerably larger than the values for the FC structures and with a trend in accordance to the electron lone-pairs screening of the electronic interaction.

Excited states with the highest oscillator strengths for the naphthalene dimers correspond to $\pi\rightarrow\pi^*$ excitations localized on one naphthalene or to mixing between $\pi\rightarrow\pi^*$ and $n(SO_n)\rightarrow\pi^*$ (**D0** and **D1**) excitations. Computed vertical emission energies and Stokes shifts for these states are in very good agreement with experimental measurements. The **D1** dimer also exhibits *syn* and *anti* low-lying states with virtually pure CT_B character and small oscillator strengths. Emission energies for $n(SO_n),\pi\rightarrow\pi^*$ (L) states are in very good agreement with photoluminescence frequencies and intensities computed by model systems with only one naphthalene unit (Table S3), confirming the localized nature of the transition.

Table 3. Vertical deexcitation energy ΔE (in eV), oscillator strength *f*, Stokes shift (in eV) and electronic character for the most stable conformers of **D0**, **D1** and **D2** dimers computed at the ωB97X-D/6-31+G(d) level. Relative stabilities between optimized excited states ΔE(rel) are also given (in kcal/mol). Labels in parenthesis for transitions involving π-type orbitals indicate localization on one naphthalene unit (L), delocalization over both naphthalene moieties (D) and excimer state nature (E).

dimer	*conf.*	character	ΔE(em)[a]	*f*	ΔE(Stokes)[b]	ΔE(rel)
D0	*syn*	π→π* (E)	3.12	0.110	1.12	6.7
	syn	*n*(S),π→π* (L)	3.58	0.316	0.66	1.9
	anti	*n*(S),π→π* (L)	3.39	0.215	0.85	2.6
	syn	*n*(S),π→π* (D)	3.51	0.325	0.73	2.1
	anti	*n*(S),π→π* (D)	3.43	0.322	0.81	0.0
D1	*syn*	π→π* (E)	2.95	0.078	1.45	0.0
	syn'	π→π* (E)	2.88	0.070	1.52	1.1
	anti	*n*(SO),π→π* (L)	3.65	0.191	0.76	3.7
	perp.	*n*(SO),π→π* (L)	3.42	0.238	0.99	4.3
	perp.'	*n*(SO),π→π* (L)	3.23	0.167	1.18	3.6
	syn	*n*(SO)→π* (D)	3.06	0.004	1.35	2.9
	anti	*n*(SO)→π* (D)	3.02	0.019	1.39	2.8
D2	*syn*	π→π* (E)	2.92	0.077	1.50	0.0
	anti	π→π* (L)	3.69	0.217	0.74	3.7
	perp.	π→π* (L)	3.78	0.262	0.65	6.4

[a]Experimental emission maxima was obtained at 3.37 eV for the three dimers, while the measured Stokes shift was 0.74, 0.82 and 0.79 eV for **D0**, **D1** and **D2**, respectively.[9]
[b]Computed Stokes shift with respect to the vertical absorption of the most stable ground state conformer.

Excited state PES along the molecular relative torsion between the two naphthalene moieties of **Dn** dimers exhibit similar energy profiles to the ground state PES, with energy barriers for the conversion between different conformers within the 2-7 kcal/mol range (Figures S2-S4). The energy profiles of S_0 and S_1 PES around the ground state local minima are rather parallel, suggesting that, depending on the experimental excitation conditions, two limiting situations might arise: (i) initial excitation does not modify the conformer population and the emitting states are entirely controlled by the ground state equilibria, or (b) the final emitting states are dictated by the relative stabilities between the minima in the S_1 PES (*excited state equilibria*). The latter situation would be closer to the case with excitation energies high enough to surpass torsion barriers. Simulated emission spectra in DCM for the two limiting situations are shown in Figure 4.

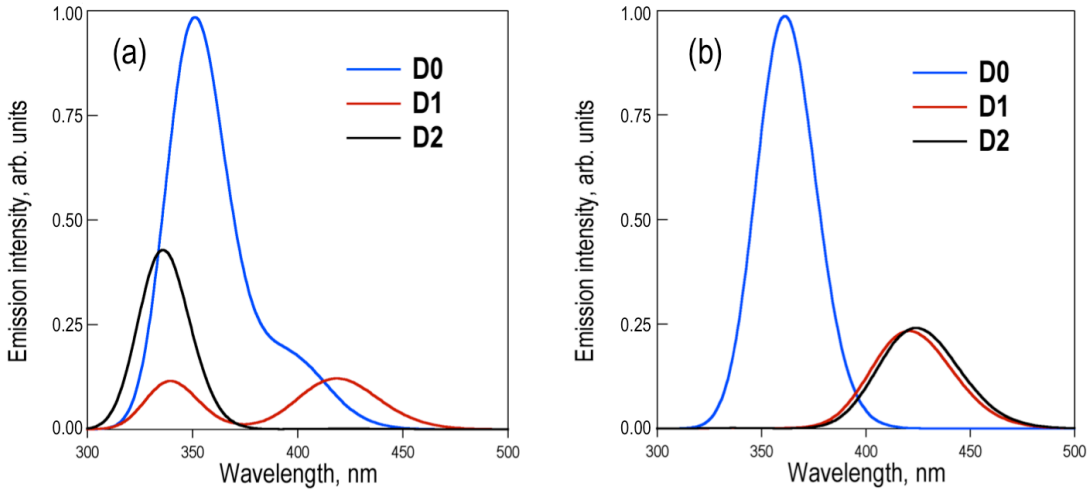

Figure 4. Simulation of emission spectra of **D0**, **D1** and **D2** dimers in DCM solution averaged over the ground state (a) and excited state (b) populations. Note that non-radiative decays have not been considered in the simulations.

Estimation of relative photoluminescence (PL) quantum yields obtained from the integration of the emission profiles (Table S5), either considering ground or excited state Boltzmann populations (Figure 4a and 4b respectively), indicate **D0** dimer as the stronger emitter with a fluorescent efficiency being three to four times larger than in **D1** and **D2**. This result is in complete disagreement to experimental observations, i.e. much larger PL quantum yield (about one order of magnitude or more) in **D2** with respect to **D0** and **D1** dimers.[9] At this point, we must conclude that different state distributions over the computed S_1 minima cannot account for the different PL efficiencies between the sulfur-bridged naphthalene dimers, and that one or more non-radiative relaxation pathways (not considered so far) might play an important role in the deactivation of **D0** and **D1** dimers. In the following, we explore potential non-radiative $S_1 \rightarrow S_0$ decays and rationalize how these mechanisms are favored in **D0** and **D1**, but not in **D2**, resulting in much larger emission intensity in the latter.

3.4. Non-radiative relaxation pathways

Firstly, we consider the possibility of efficient internal conversion (IC) of **D1** dimer following the pyramidal inversion mechanism on the excited state PES, as it has been proposed as a viable photo-induced process in aryl sulfoxides.[30] The energy barriers computed for the inversion of the *syn* and *anti* **D1** conformers are 3.5 and 3.0 kcal/mol, much lower than the energy required for the same structural rearrangement in the ground state (39 kcal/mol). Hence, it seems that the inversion might be thermally available after photo-excitation of the sulfoxide dimer. But, in order for such a mechanism to result in an efficient IC to the ground state, strong non-adiabatic coupling between the two states is required. Since

the interstate couplings are inversely proportional to the energy gap, a small energy difference between the two PESs is necessary. Estimation of the S_0/S_1 energy gaps at the inversion TS are computed as 32 and 50 kcal/mol for the *syn* and *anti* conformers, respectively (Table S6). Hence, despite the availability of the photo-induced pyramidal inversion in **D1**, the magnitude of the S_0/S_1 gaps forces us to rule out the efficient non-radiative decay via IC at the inversion TS. Although the computed tetrahedral inversion barrier for **D2** in the lowest excited state is also considerably much lower than the ground state value, i.e. 41 vs. 97 kcal/mol, in this case the barrier is still too large to allow for photo-induced tetrahedral inversion. Furthermore, the S_0/S_1 energy gap at the TS is estimated at 29 kcal/mol, blocking the non-radiative decay to the ground state via IC. Similar results have been obtained for the energy difference between the two states of **D0** at the inversion TS, i.e. 14 kcal/mol and 11 kcal/mol for the *syn* and *anti* conformers, respectively.

In an attempt to find potential efficient non-radiative mechanisms for the photo-excited naphthalene dimers, we explore regions of the PES where the gap between the ground and lowest excited singlet state becomes small or where the two states become degenerate, that is S_0/S_1 intersections. For the sake of clarity, in the following we only discuss the results regarding the most stable conformations, that is *syn* (**D0** and **D1**) and *anti* (**D2**) forms. Motivated by the lowering of the S_0/S_1 gap at the TS of the pyramidal inversion for **D1**, we search for energy crossings from the trigonal planar arrangement of the SO_1 bridge. Indeed, we identify a molecular geometry structurally related to the TS where the ground and excited PES intersect with non-vanishing non-adiabatic couplings at the proximity of the crossing (Supporting Information), i.e. a conical intersection (CI). At this intersection that we label as *sym*-CI, there is a symmetric elongation of the S-C bonds between SO_1 and naphthalene units and an important increase of the bridge C-S-C angle (Table 4). More importantly, the *sym*-CI point lies ~0.66 eV below the S_1 state at the FC region, thus it is energetically accessible upon photo-excitation, providing a clear molecular mechanism to relax back to ground state without photoemission. Similarly, we obtain a symmetric state crossing for the **D0** dimer, which exhibits a similar geometrical pattern (long C-S bonds and linear C-S-C angle). But, in this case, the *sym*-CI is obtained energetically above the FC S_1 energy. For both dimers, **D0** and **D1**, at the *sym*-CI the ground state crosses with the $n(SO_n)\rightarrow\sigma^*$ state, which is stabilized by the elongation of the two S-C bonds (Figure 5). Moreover, in **D1**, the planarization of the sulfoxide group destabilizes the n(SO) due to π anti-bonding interaction with the p_z orbital of the oxygen atom. In the **D0** dimer, the n(S) destabilization comes from the interaction with the π-orbitals of coplanar naphthalene fragments. On the other hand, the lack of electron lone-pairs in the sulfone bridge inhibits the presence of low energy *sym*-CI in the **D2** dimer.

Table 4. Structural parameters (in Å and degrees) and relative energies (in eV) with respect to the S_1 energy at the FC region of the inversion TS (*inv*-TS), and the *sym*-CI and the *asym*-CI points for the *syn* conformers of **D0** and **D1** dimers.[a]

dimer	*state*	*r*(C-S)	α(C-S-C)	ΔE(rel)
D0	*inv*-TS	1.80/1.80	178	+0.60
	sym-CI	2.17/2.12	178	+0.68
	asym-CI	2.26/1.77	176	-0.23
D1	*inv*-TS	1.76/1.76	115	+0.15
	sym-CI	1.96/1.88	155	-0.66
	asym-CI	2.32/1.78	107	-1.03

[a]Geometries for the *sym*-CI and *asym*-CI can be found in Figure S7.

Excited state optimization within the CI subspace, i.e. minimal energy CI (MECI), of sulfide and sulfoxide dimers result in non-symmetric molecular geometries (*asym*-CI) with one rather long S···C distance and a short S-C bond. As a result, the σ* localizes on one side of the dimer (at the long S···C separation). This structural arrangement suggests a path towards molecular fragmentation. Furthermore, the computed *asym*-CI energies lie below the S_1 energy at the FC region (and below the *sym*-CI point), and are therefore energetically available for both dimers. Hence, we identify the non-adiabatic relaxation of **D0** and **D1** dimers through *asym*-CI as the mechanism describing reversible molecular fragmentation (although the molecule has not been effectively fragmented in *asym*-CI), where there is an elongation and shrinking of a S-C bond resulting in a fast decay to the electronic ground state. The reverse fragmentation mechanism has been proposed as the main inversion of aryl sulfoxides with a 1° alkyl group.[29,31,32,34] Moreover, we find that such a mechanism can be potentially photoinduced in sulfide and sulfoxide aromatic dimers and proceeds through a MECI.

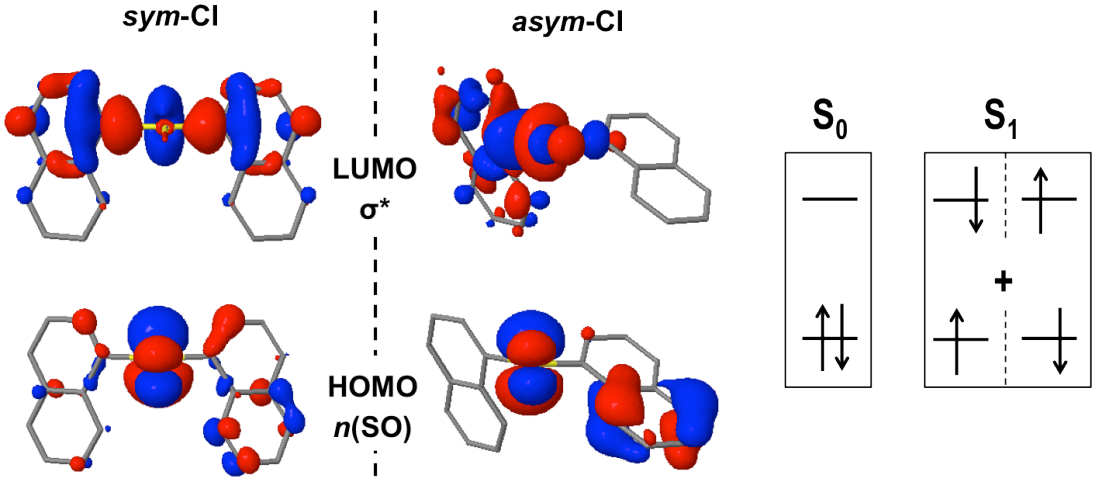

Figure 5. Frontier molecular orbitals *n*(SO) and σ* at the S_0/S_1 *sym*-CI and *asym*-CI points for the sulfoxide naphthalene dimer (**D1**).

By gathering the results discussed above regarding the photoexcitation and different deactivation paths of the studied naphthalene dimers, it is possible to draw a general picture for the photophysical properties of **Dn**. The main photophysical mechanisms explored are represented in the Jablonski diagram of Figure 6. Relaxation of the photoexcited sulfur-bridged naphthalene dimers allow the formation of strongly emissive localized excitations and weakly emitting excimers. Moreover, sulfide and sulfoxide dimers exhibit non-radiative decay back to the ground state, which actually dominate their excited state dynamics in solution. On the other hand, the lack of electron lone-pair in **D2** blocks the presence of low-lying ground-excited state crossings, resulting in much larger PL yields with respect to **D0** and **D1**.

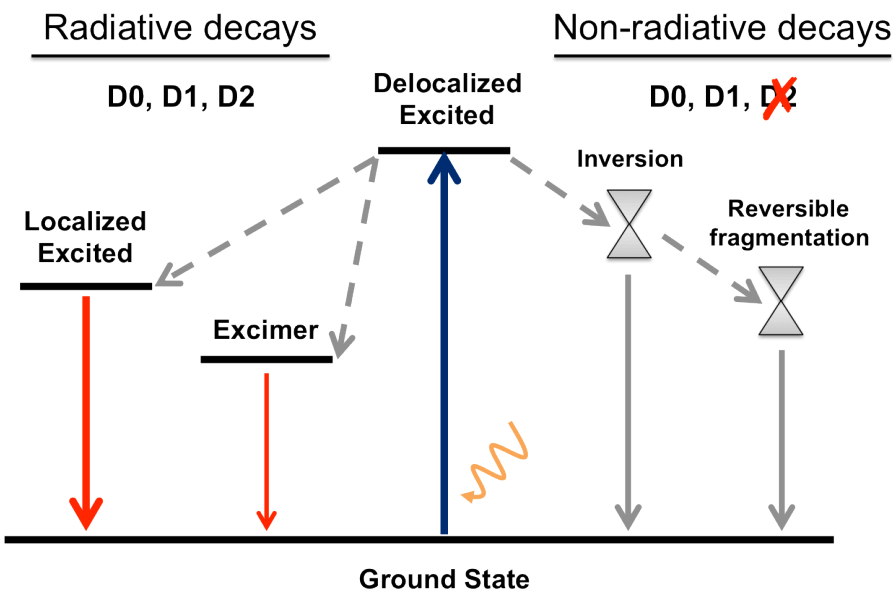

Figure 6. General Jablonski diagram for the deactivation mechanisms after photoexcitation of **D0**, **D1** and **D2** naphthalene dimers.

5. Conclusions

In this work we have identified and characterized both radiative and non-radiative deactivation mechanisms in sulfur-bridged naphthalene dimers. The different PL efficiencies upon oxidation of the bridge have been rationalized by the existence of energetically available non-radiative decays for the sulfide and sulfoxide bridges. The lack of electron lone-pairs in the sulfone linker is the origin of the much stronger PL with respect to S and SO_1 cases.

Although the computed vertical transition energies and their intensities at the FC structures are very similar for the three naphthalene dimers, there are sensible differences in the character of the transition to the lowest excited singlet between **D0**, **D1** and **D2**, that is

larger involvement of the $n(SO_n)$ orbitals in terms of bridge→naphthalene CT with lower oxidation state of the sulfur atom. Geometrical relaxation to local minima of the excited state PESs cannot account for the very weak PL of **D0** and **D1**, pointing towards the existence of efficient non-radiative decays, not present from the excited **D2**. We identify energy crossing regions in **D0** and **D1** dimers allowing the conversion of the photo-excited molecules back to the ground state with no fluorescence emission. Our calculations indicate that while two types of S_0/S_1 state crossings, i.e. symmetric and asymmetric, might be reached along the excited state decay of **D1**, only the asymmetric intersection is energetically available in the **D0** dimer. The identification of energetically available asymmetric CI pointing towards the reversible molecular fragmentation, suggests a photoinduced roaming mechanism[35] as a potential non-radiative deactivation path of **D0** and **D1**. Finally, it is important to notice that in our calculations, due to the nature of the studied chromophores, we do not have considered the role of ISC as one of the main deactivation channels.

The present results suggest that, differently to the terthiophene dimers, the SO_n bridged naphthalene bichromophores do not require efficient ISC to limit fluorescence emission. On the other hand, our results reinforce the generality of the electron lone-pair screening concept for sulfur-bridged chromophore dimers. The obtained results and conclusion are general enough to be extrapolated to other sulfur-bridged conjugated dimers, therefore proportionating novel strategies in the design of strong photoluminescence organic molecules with controlled charge transfer. Investigations in this direction are currently in pursuit in our labs.

6. Acknowledgements

We are grateful to Professors Pere Alemany and Josep Maria Bofill, and Dr. Miquel Huix-Rotllant for valuable insight and fruitful discussions. This work has been supported by the Basque Government (project IT588-13) and the Spanish Government MINECO/FEDER (projects CTQ2016-80955 and CTQ2015-64579-C3-3-P). D.C. thanks IKERBASQUE, Basque Foundation for Science for financial support. C.C. is indebted to the Spanish "Ministerio de Economía y Competitividad" for a predoctoral FPI grant and an EEBB mobility grant for a research stay in Marseille. M.B. thanks the support of the A*MIDEX grant (n° ANR-11-IDEX-0001-02) and of the project Equip@Meso (ANR-10-EQPX-29-01), both funded by the French Government "Investissements d'Avenir" program.

7. References

(1) Heliatek, http://www.heliatek.com.
(2) NREL Best Research-Cell Efficiencies, http://www.nrel.gov/ncpv/images/efficiency_chart.jpg.
(3) Rettig, W. Charge Separation in Excited States of Decoupled Systems—TICT Compounds and Implications Regarding the Development of New Laser Dyes and the Primary Process of Vision and Photosynthesis. *Angew. Chem. Int. Ed.* **1986**, *25*, 971.
(4) Grabowski, Z. R.; Rotkiewicz, K.; Rettig, W. Structural Changes Accompanying Intramolecular Electron Transfer: Focus on Twisted Intramolecular Charge-Transfer States and Structures. *Chem. Rev.* **2003**, *103*, 3899.
(5) Bartynski, A. N.; Gruber, M.; Das, S.; Rangan, S.; Mollinger, S.; Trinh, C.; Bradforth, S. E.; Vandewal, K.; Salleo, A.; Bartynski, R. A.; Bruetting, W.; Thompson, M. E. Symmetry-Breaking Charge Transfer in a Zinc Chlorodipyrrin Acceptor for High Open Circuit Voltage Organic Photovoltaics. *J. Am. Chem. Soc.* **2015**, *137*, 5397.
(6) Fyfe, D. LED Technology: Organic displays come of age. *Nat. Photon.* **2009**, *3*, 453.
(7) Santato, C.; Cicoira, F.; Martel, R. Organic photonics: Spotlight on organic transistors. *Nat. Photon.* **2011**, *5*, 392.
(8) Kulkarni, A. P.; Tonzola, C. J.; Babel, A.; Jenekhe, S. A. Electron Transport Materials for Organic Light-Emitting Diodes. *Chem. Mater.* **2004**, *16*, 4556.
(9) Christensen, P. R.; Nagle, J. K.; Bhatti, A.; Wolf, M. O. Enhanced Photoluminescence of Sulfur-Bridged Organic Chromophores. *J. Am. Chem. Soc.* **2013**, *135*, 8109.
(10) Cruz, C. D.; Christensen, P. R.; Chronister, E. L.; Casanova, D.; Wolf, M. O.; Bardeen, C. J. Sulfur-Bridged Terthiophene Dimers: How Sulfur Oxidation State Controls Interchromophore Electronic Coupling. *J. Am. Chem. Soc.* **2015**, *137*, 12552.
(11) Becker, R. S.; Seixas de Melo, J.; Maçanita, A. L.; Elisei, F. Comprehensive Evaluation of the Absorption, Photophysical, Energy Transfer, Structural, and Theoretical Properties of α-Oligothiophenes with One to Seven Rings. *J. Phys. Chem.* **1996**, *100*, 18683.
(12) Rossi, R.; Ciofalo, M.; Carpita, A.; Ponterini, G. Singlet—triplet intersystem crossing in 2,2′:5′,2″-terthiophene and some of its derivatives. *J. Photochem. Photobiol., A* **1993**, *70*, 59.
(13) Parr, R. G. In *Horizons of Quantum Chemistry: Proceedings of the Third International Congress of Quantum Chemistry Held at Kyoto, Japan, October 29 - November 3, 1979*; Fukui, K., Pullman, B., Eds.; Springer Netherlands: Dordrecht, 1980, p 5.
(14) Ziegler, T. Approximate density functional theory as a practical tool in molecular energetics and dynamics. *Chem. Rev.* **1991**, *91*, 651.
(15) Casida, M. E. *Time-dependent density-functional response theory for molecules*; World Scientific: Singapure, 1995; Vol. 1.
(16) Runge, E.; Gross, E. K. U. Density-Functional Theory for Time-Dependent Systems. *Phys. Rev. Lett.* **1984**, *52*, 997.
(17) Chai, J.-D.; Head-Gordon, M. Long-range corrected hybrid density functionals with damped atom-atom dispersion corrections. *Phys. Chem. Chem. Phys.* **2008**, *10*, 6615.
(18) Hariharan, P. C.; Pople, J. A. The influence of polarization functions on molecular orbital hydrogenation energies. *Theor. Chim. Acta* **1973**, *28*, 213.
(19) Franci, M. M.; Pietro, W. J.; Hehre, W. J. Self-consistent molecular orbital methods. XXIII. A polarization-type basis set for second-row elements. *J. Chem. Phys.* **1982**, *77*, 3654.
(20) Clark, T.; Chandrasekhar, J.; Spitznagel, G. W.; Schleyer, P. V. R. Efficient diffuse function-augmented basis sets for anion calculations. III. The 3-21+G basis set for first-row elements, Li–F. *J. Comput. Chem.* **1983**, *4*, 294.
(21) Chipman, D. M. Reaction field treatment of charge penetration. *J. Chem. Phys.* **2000**, *112*, 5558.
(22) Cancès, E.; Mennucci, B. Comment on "Reaction field treatment of charge penetration" [J. Chem. Phys. 112, 5558 (2000)]. *J. Chem. Phys.* **2001**, *114*, 4744.
(23) Subotnik, J. E.; Cave, R. J.; Steele, R. P.; Shenvi, N. The initial and final states of electron and energy transfer processes: Diabatization as motivated by system-solvent interactions. *J. Chem. Phys.* **2009**, *130*, 234102.
(24) Shao, Y.; Head-Gordon, M. The spin–flip approach within time-dependent density functional theory: Theory and applications to diradicals. *J. Chem. Phys.* **2003**, *118*, 4807.

(25) Becke, A. D. Density-functional exchange-energy approximation with correct asymptotic behavior. *Phys. Rev. A* **1988**, *38*, 3098.
(26) Lee, C.; Yang, W.; Parr, R. G. Development of the Colle-Salvetti correlation-energy formula into a functional of the electron density. *Phys. Rev. B* **1988**, *37*, 785.
(27) Frisch, M. J.; Trucks, G. W.; Schlegel, H. B.; Scuseria, G. E.; Robb, M. A.; Cheeseman, J. R.; Scalmani, G.; Barone, V.; Mennucci, B.; Petersson, G. A.; Nakatsuji, H.; Caricato, M.; Li, X.; Hratchian, H. P.; Izmaylov, A. F.; Bloino, J.; Zheng, G.; Sonnenberg, J. L.; Hada, M.; Ehara, M.; Toyota, K.; Fukuda, R.; Hasegawa, J.; Ishida, M.; Nakajima, T.; Honda, Y.; Kitao, O.; Nakai, H.; Vreven, T.; Montgomery Jr., J. A.; Peralta, J. E.; Ogliaro, F.; Bearpark, M. J.; Heyd, J.; Brothers, E. N.; Kudin, K. N.; Staroverov, V. N.; Kobayashi, R.; Normand, J.; Raghavachari, K.; Rendell, A. P.; Burant, J. C.; Iyengar, S. S.; Tomasi, J.; Cossi, M.; Rega, N.; Millam, N. J.; Klene, M.; Knox, J. E.; Cross, J. B.; Bakken, V.; Adamo, C.; Jaramillo, J.; Gomperts, R.; Stratmann, R. E.; Yazyev, O.; Austin, A. J.; Cammi, R.; Pomelli, C.; Ochterski, J. W.; Martin, R. L.; Morokuma, K.; Zakrzewski, V. G.; Voth, G. A.; Salvador, P.; Dannenberg, J. J.; Dapprich, S.; Daniels, A. D.; Farkas, Ö.; Foresman, J. B.; Ortiz, J. V.; Cioslowski, J.; Fox, D. J.; Gaussian, Inc.: Wallingford, CT, USA, 2009.
(28) Shao, Y.; Gan, Z.; Epifanovsky, E.; Gilbert, A. T. B.; Wormit, M.; Kussmann, J.; Lange, A. W.; Behn, A.; Deng, J.; Feng, X.; Ghosh, D.; Goldey, M.; Horn, P. R.; Jacobson, L. D.; Kaliman, I.; Khaliullin, R. Z.; Kuś, T.; Landau, A.; Liu, J.; Proynov, E. I.; Rhee, Y. M.; Richard, R. M.; Rohrdanz, M. A.; Steele, R. P.; Sundstrom, E. J.; Woodcock, H. L.; Zimmerman, P. M.; Zuev, D.; Albrecht, B.; Alguire, E.; Austin, B.; Beran, G. J. O.; Bernard, Y. A.; Berquist, E.; Brandhorst, K.; Bravaya, K. B.; Brown, S. T.; Casanova, D.; Chang, C.-M.; Chen, Y.; Chien, S. H.; Closser, K. D.; Crittenden, D. L.; Diedenhofen, M.; DiStasio, R. A.; Do, H.; Dutoi, A. D.; Edgar, R. G.; Fatehi, S.; Fusti-Molnar, L.; Ghysels, A.; Golubeva-Zadorozhnaya, A.; Gomes, J.; Hanson-Heine, M. W. D.; Harbach, P. H. P.; Hauser, A. W.; Hohenstein, E. G.; Holden, Z. C.; Jagau, T.-C.; Ji, H.; Kaduk, B.; Khistyaev, K.; Kim, J.; Kim, J.; King, R. A.; Klunzinger, P.; Kosenkov, D.; Kowalczyk, T.; Krauter, C. M.; Lao, K. U.; Laurent, A. D.; Lawler, K. V.; Levchenko, S. V.; Lin, C. Y.; Liu, F.; Livshits, E.; Lochan, R. C.; Luenser, A.; Manohar, P.; Manzer, S. F.; Mao, S.-P.; Mardirossian, N.; Marenich, A. V.; Maurer, S. A.; Mayhall, N. J.; Neuscamman, E.; Oana, C. M.; Olivares-Amaya, R.; O'Neill, D. P.; Parkhill, J. A.; Perrine, T. M.; Peverati, R.; Prociuk, A.; Rehn, D. R.; Rosta, E.; Russ, N. J.; Sharada, S. M.; Sharma, S.; Small, D. W.; Sodt, A. Advances in molecular quantum chemistry contained in the Q-Chem 4 program package. *Mol. Phys.* **2015**, *113*, 184.
(29) Cubbage, J. W.; Jenks, W. S. Computational Studies of the Ground and Excited State Potentials of DMSO and H2SO: Relevance to Photostereomutation. *J. Phys. Chem. A* **2001**, *105*, 10588.
(30) Kathayat, R. S.; Yang, L.; Sattasathuchana, T.; Zoppi, L.; Baldridge, K. K.; Linden, A.; Finney, N. S. On the Origins of Nonradiative Excited State Relaxation in Aryl Sulfoxides Relevant to Fluorescent Chemosensing. *J. Am. Chem. Soc.* **2016**, *138*, 15889.
(31) Mislow, K.; Axelrod, M.; Rayner, D. R.; Gotthardt, H.; Coyne, L. M.; Hammond, G. S. Light-Induced Pyramidal Inversion of Sulfoxides1. *J. Am. Chem. Soc.* **1965**, *87*, 4958.
(32) Guo, Y.; Jenks, W. S. Photolysis of Alkyl Aryl Sulfoxides: α-Cleavage, Hydrogen Abstraction, and Racemization1. *J. Org. Chem.* **1997**, *62*, 857.
(33) Lindquist, B. A.; Woon, D. E.; Dunning, T. H. Electronic Structure of H2S, SF2, and HSF and Implications for Hydrogen-Substituted Hypervalent Sulfur Fluorides. *J. Phys. Chem. A* **2014**, *118*, 1267.
(34) Vos, B. W.; Jenks, W. S. Evidence for a Nonradical Pathway in the Photoracemization of Aryl Sulfoxides1. *J. Am. Chem. Soc.* **2002**, *124*, 2544.
(35) Suits, A. G. Roaming Atoms and Radicals: A New Mechanism in Molecular Dissociation. *Acc. Chem. Res.* **2008**, *41*, 873.